

Diffusion-reaction mechanisms of nitriding species in SiO₂

W. Orellana,* Antônio J. R. da Silva, and A. Fazzio

Instituto de Física, Universidade de São Paulo, C.P. 66318, 05315-970, São Paulo, SP, Brazil

(Received 27 November 2003; revised manuscript received 23 March 2004; published 16 September 2004)

We study using first-principles total-energy calculations, diffusion-reaction processes involved in the thermal nitridation of SiO₂. We consider NO, NH, N₂, and atomic N in different charge states as the nitriding species in α -quartz. Our results show that none of neutral species react with the SiO₂ network remaining at interstitial sites. Therefore, they are likely to diffuse through the oxide, incorporating nitrogen at near-interface (Si-SiO₂) regions. Whereas, charged species are trapped by the network, nitriding bulk SiO₂. For the diffusing species, we find that NH and atomic N show increasing diffusivities with temperatures, whereas for NO and N₂ they are relatively constant. This result agrees well with the finding of higher N concentrations at the Si-SiO₂ interface obtained by thermal processing of SiO₂ in NH₃ as compared with those obtained in N₂O. Finally, we discuss spin-dependent incorporation reaction mechanisms of NH and atomic N with the SiO₂ network.

DOI: 10.1103/PhysRevB.70.125206

PACS number(s): 71.55.Ht, 71.15.Nc, 71.15.Mb, 66.30.Ny

I. INTRODUCTION

Nitrided silicon oxide or oxynitride is currently the near-term solution to substitute SiO₂ as the gate insulator material for the ultrathin metal-oxide-semiconductors (MOS) technology. Recent studies have suggested that the performance of oxynitride-based MOS devices depends both on the depth concentration and on the distribution of nitrogen into the gate oxide.¹ According to these studies, the best nitrogen profile for an ultrathin gate oxide would have: (i) a small nitrogen concentration near the SiO₂-Si interface in order to reduce degradations by hot electrons,² and (ii) a larger N concentration near the interface between the dielectric and the polycrystalline silicon (poly-Si) gate electrode, in order to minimize dopant diffusion.³

The growth of ultrathin oxynitride films depends strongly on the reactant agent (e.g., N₂O, NO, NH₃) and the technique used. Nitrogen can be incorporated into SiO₂ using either thermal oxidation and annealing or chemical and physical deposition methods. Thermal nitridation of SiO₂ in N₂O generally results in a relatively low N concentration at near-interface (Si-SiO₂) region. The nitriding species are originated in the decomposition of the N₂O molecule occurring at typical oxidation temperature, these species being the NO and N₂ molecules.⁴⁻⁶ On the other hand, nitrogen incorporation in SiO₂ can also be performed via annealing in a NH₃ atmosphere, resulting in a relatively high N concentrations into the films.⁵ This method provides both near-interface and near-surface nitridation, which suggests different mechanisms for N incorporation or different nitriding species derived from NH₃. The above thermal processing are performed at high temperatures (>800 °C). Plasma nitridation is a promising method for making ultrathin oxynitride at lower temperatures (~300–400 °C). Higher N concentrations and controlled distribution can be attained with this method,⁷ typically using ions and radicals derived from N₂ and NH₃ as nitrogen sources.⁸ Additionally, nitridation by energetic particles (N ions) provides high N concentrations much closer to the near-surface region, with little or no ni-

trogen at the SiO₂-Si interface.¹ Although the nitridation mechanisms to make ultrathin oxynitride films are well known at the few layer level, less is known about the diffusing mechanism of the nitriding species and their reactions with the oxide at the atomic level. Recently, the stability and electronic properties of nitrogen incorporation in suboxide SiO₂ have been studied from theoretical calculations.⁹ In this work has been suggested that nitriding species like NO and atomic N would introduce trapping centers after reacting with Si-Si bonds at the Si-SiO₂ interface. Whereas, NH would improve the electrical reliability of oxynitride films.¹⁰

In this work the energetics and diffusing properties of the SiO₂ thermal nitridation are studied from first-principles total-energy calculations. We have considered the N₂, NH, and NO molecules as well as atomic N in different charge states as the nitriding species reacting and diffusing through the SiO₂ network. The outline of the paper is as follows. Section II describes the theoretical procedure. Our results for the interaction of the nitriding species with the SiO₂ network is presented in Sec. III A. The diffusivity of the nitriding species through SiO₂ is presented in Sec. III B. In Sec. III C we discuss the spin-dependent diffusion reactions of NH and atomic N with the SiO₂ network. Finally, in Sec. IV we show our conclusions.

II. THEORETICAL METHOD

Our calculations were performed in the framework of the density functional theory,¹¹ using a basis set of numerical atomic orbitals as implemented in the SIESTA code.¹² We have used a split-valence double- ζ basis set plus the polarization functions, and standard norm-conserving pseudopotentials to describe the electron-ion interaction.¹³ For the exchange-correlation potential we adopt the generalized gradient approximation.¹⁴ We used a 72-atom α -quartz supercell and the Γ point for the Brillouin zone sampling. The positions of all the atoms in the supercell were relaxed until all the force components were smaller than 0.05 eV/Å. We also

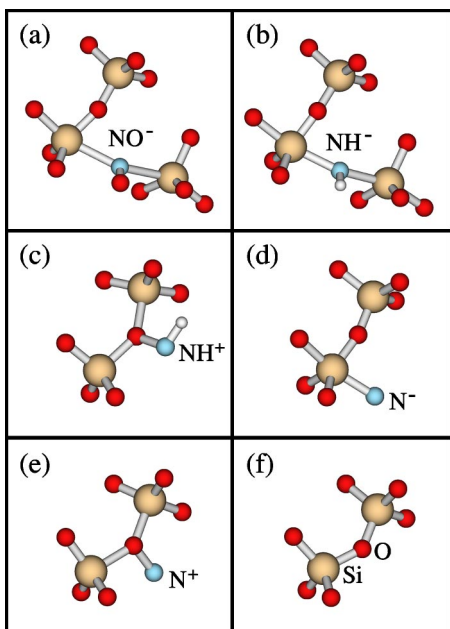


FIG. 1. Local equilibrium geometries for singly charged nitriding species after reacting with the SiO₂ network. (a) Negative NO; (b) negative and (c) positive NH, respectively; (d) negative and (e) positive atomic N, respectively; (f) the perfect SiO₂ network.

consider neutral and singly charged species, where the neutrality of the cell is always maintained by introducing a compensating background charge. Spin-polarization effects are included throughout the calculation since they are important for the correct description of atomic and molecular reaction processes in SiO₂.¹⁵ We initially study the energetics and structural properties of N₂, NH, NO, and atomic N in the largest interstitial site of α -quartz for three different charge states (+, 0, -). We explore possible reactions that these species may undergo with the network as well as their diffusivities in α -quartz.

III. RESULTS AND DISCUSSION

A. Incorporation of nitriding species into the SiO₂ network

Thermal processing of SiO₂ in N₂O and NO atmospheres shows that the NO molecule is the species which diffuses through the oxide, being incorporated at the Si-SiO₂ interface.⁶ In our calculations we find that neutral NO and NO⁺ do not react chemically with the SiO₂ network, remaining at the interstitial positions. We verify an electrostatic repulsion when the molecules are forced to approach to the network. Thus, neutral NO and NO⁺ would be diffusing species in the oxide. On the contrary, the interstitial NO⁻ molecule is trapped by the perfect SiO₂ network, forming a structure where the N atom of the molecule is bound to two Si atoms of SiO₂, as shown in Fig. 1(a). The binding energy of NO⁻, calculated as the difference in energy between the bound and the free-interstitial configurations for the same charge state, is found to be 1.3 eV. The N-O and both Si-N bond lengths are 1.23 and 2.26 Å, respectively, whereas the

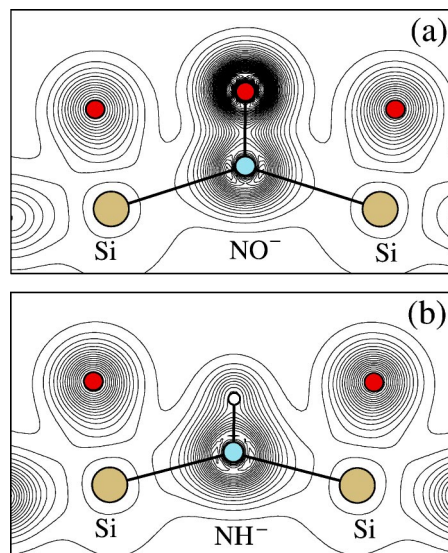


FIG. 2. Charge density contour plots for interstitial molecules binding with the SiO₂ network: (a) Negative NO, and (b) negative NH. The total charge density is plotted in a plane that passes through the the Si-[NO]-Si and Si-[NH]-Si equilibrium structures. In both plots the outermost contour line and the contour spacing are $0.2 e/\text{\AA}^3$.

distance between the Si atoms in the Si-[NO]-Si configuration decreases by about 6% with respect to those of perfect SiO₂. For interstitial NO and NO⁺ the N-O bond lengths are 1.17 and 1.13 Å, respectively. Figure 2(a) shows the charge density contour plots of NO⁻ at the equilibrium interstitial configuration binding with the SiO₂ network. The total charge density is plotted in a plane that passes through the Si-[NO]-Si structure. Here, we observe that the interaction between the Si atoms and NO⁻ is mainly electrostatic, without charge transfer between them. The highly electronegative molecule is attracted by the cation-like Si atoms.

The NH radical seems to be the most likely diffusing species after thermal dissociation of NH₃ according to the dissociative reactions: NH₃ → NH₂ + H - 4.5 eV and NH₂ → NH + H - 3.9 eV. Although NH₂ may be another diffusing species for the interface nitridation, it is a relatively larger molecule and it may suffer additional dissociations at near-surface SiO₂ during thermal processing. According to our results, neutral NH in the gas phase has a spin triplet ($S=1$) ground state whereas the singlet ($S=0$) states is 2.06 eV higher in energy. However, inside the largest interstitial site of α -quartz, this difference in energy between both spin configurations decreases to 1.04 eV, due to the interaction with the crystal field. We find that triplet NH does not react chemically with the SiO₂ network remaining relatively inert at the interstitial sites. However, singlet NH reacts quickly with the oxide forming a structure where the N atom of NH forms a strong bond with an O atom of the oxide as shown in Fig. 3(a). This incorporation reaction is highly exothermic with an energy gain of 2.04 eV. In Sec. III C we discuss the possibility that NH might be incorporated in the SiO₂ network via a triplet-to-singlet spin exchange.

Singly charged NH molecules are highly reactive in the SiO₂ network, forming bound configurations as shown in

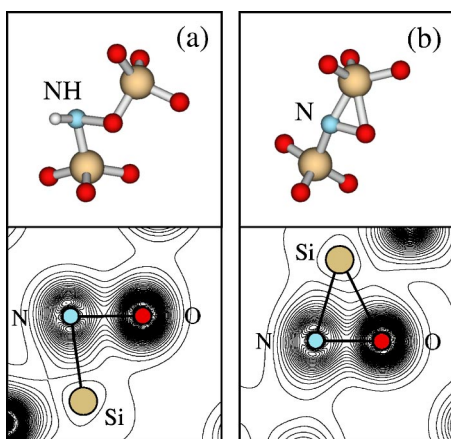


FIG. 3. Equilibrium geometries and total charge densities for neutral NH and atomic N in their excited spin configurations, after being incorporated into the SiO_2 network. (a) Singlet NH ($S=0$) (b) doublet N ($S=1/2$). The charge densities are plotted in a plane that passes through the Si-N-O bonding structure. In both plots the outermost contour line and the contour spacing are $0.2 e/\text{\AA}^3$.

Figs. 1(b) and 1(c). The binding energies for NH^- and NH^+ are 3.2 and 2.7 eV, respectively, which suggest that these configurations are very stable favoring a SiO_2 near-surface nitridation. In the NH^+ bound configuration [Fig. 1(c)], the N atom binds to an O atom of the oxide keeping its bond to the H atom. The O-N and N-H bond lengths are 1.43 and 1.05 \AA , respectively, forming a O-N-H angle of 103° . The equilibrium configuration of interstitial NH^- is similar to that previously found for NO^- . However, the relaxation of the SiO_2 network is larger for the NH^- bound configuration [see Fig. 1(b)]. Here, both Si-N bond lengths are about 2.1 \AA , whereas the distance between the Si atoms in the Si-[NH]-Si configuration decreases by about 14% with respect to those of perfect SiO_2 , showing a larger lattice relaxation. The N-H bond length is found to be 1.04 \AA . Figure 2(b) shows the charge density contour plots of NH^- at the equilibrium interstitial configuration binding with the SiO_2 network. The total charge density is plotted in a plane that passes through the Si-[NH]-Si structure. Here, we see that the interaction between the SiO_2 network and NH^- is not only electrostatic, exhibiting also a small charge transfer from the molecule to the Si atoms. This can be verified by the increasing charge at the Si-N bonds as compared with NO^- [Fig. 2(a)], which also explain the higher binding energy of NH^- .

The N_2 molecule is a product of the N_2O gas decomposition at typical oxidation temperatures, being introduced in this way into SiO_2 in thermal processing.¹ N_2 (and atomic N) may also be introduced at lower temperatures by plasma assisted methods.⁷ Our results for N_2 in SiO_2 show that this molecule does not react with the oxide being relatively inert for the three charge states considered. Therefore, it may diffuse easily through the oxide reacting with the silicon at the Si- SiO_2 interface or escaping from the films.

The N atom in free space has a quartet ($S=3/2$) ground state. The difference in energy with respect to the doublet ($S=1/2$) state is calculated to be ~ 3 eV. However, for a N atom in the largest interstitial site of α -quartz, this energy difference decreases to 0.76 eV. We find that quartet N does

not react chemically with the SiO_2 network suggesting that it would be a diffusing species. However, doublet N reacts quickly with the oxide network forming a strong N-O bond, suggesting the reconstruction of the NO molecule, as shown in Fig. 3(b). This reaction is exothermic with an energy gain of 0.76 eV. In Sec. III C, we discuss the possibility that atomic N might be incorporated in the SiO_2 network via a quartet-to-doublet spin exchange.

Singly charged N atoms are also highly reactive in SiO_2 . N^- binds to a fourfold coordinate Si atom forming an additional Si-N bond of 1.85 \AA , as shown in Fig. 1(d). The N atom has a binding energy of 2.2 eV. On the other hand, N^+ binds to an oxygen forming a O-N bond, as shown in Fig. 1(e). We find a O-N bond length of 1.39 \AA with a N binding energy of 1.1 eV.

As a general trend, we can say that because of the ionic character of SiO_2 , charged species are bound to the network. The positively (negatively) charged NO, NH, and N species attach to anion-like O (cation-like Si) atoms of the oxide, forming strong bonds, with binding energies ranging from 1 to 3 eV. This suggests a mechanism for the high-density bulk and near-surface nitridation. On the other hand, the neutral species in their ground-state spin configurations do not react chemically with the SiO_2 network. Therefore, they are able to diffuse through the oxide.

B. Diffusion of nitriding species in SiO_2

We calculate the diffusion coefficient for the neutral species migrating through the larger channel of α -quartz, normal to the c -axis. To calculate the potential-energy surface (PES) through this channel, we have followed the same procedure as described in our previous calculation of the O_2 diffusion in α -quartz.¹⁶ Initially, we fix one atom of the species at several points along the pathway joining neighboring interstitial sites of α -quartz in order to find the barriers. Afterwards, the constraint is removed, allowing the species to evolve freely from the saddle points to the minima. Our results for the total-energy variations along the diffusion path are shown in Fig. 4. The zero distance in the figure indicates approximately the center of the largest interstitial site of alpha-quartz. The distance between equivalent neighboring interstitial sites is ~ 5 \AA . We have estimated the uncertainty in our calculated energy barriers of about 0.1 eV, typically the difference in energy of the species at equivalent interstitial sites. As a general trend, we find an anisotropic energy profile through the migration path which can be associated to the asymmetry of the channel at connecting voids. Figure 4(a) shows the calculated total-energy variations of diffusing NO and N_2 . We observe that these species show similar global minima and barrier heights, however, the N_2 PES exhibits two plateau regions along its PES, suggesting metastable positions for N_2 . These regions correspond to the closest approach of N_2 passing between two opposite Si atoms of SiO_2 , indicated by arrows in Fig. 4. Therefore, we can associate the plateau regions along the N_2 PES to cation-like regions, which are likely to accommodate this molecule. Whereas, the top of the barriers corresponds to anion-like regions where N_2 passes closest to O atoms of SiO_2 , increas-

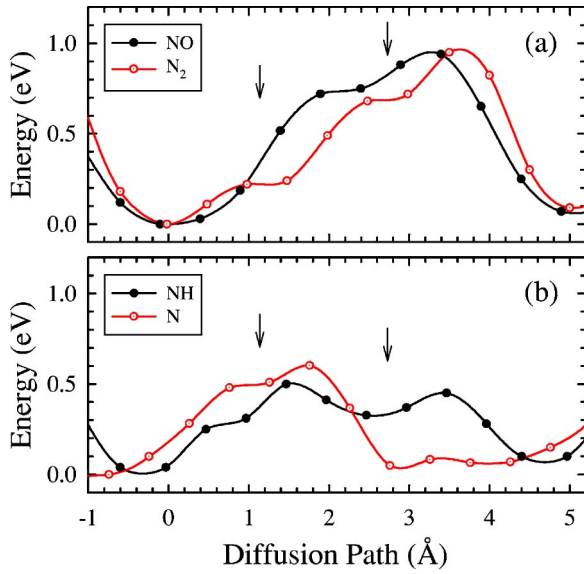


FIG. 4. Total energy variations for the neutral nitriding species diffusing through a channel normal to the c -axis of α -quartz. (a) for the NO and N_2 molecules. (b) for the NH molecule and atomic N. The arrows indicate the closest approach of the diffusing species passing between two opposite Si atoms of the network. The zero distance is the center of the largest void in α -quartz.

ing the electron clouds overlap. The other species also show similar metastabilities. Figure 4(b) shows the calculated PES for NH and atomic N. Here, we find lower energy barriers and shorter distances between minima, as compared with NO and N_2 , suggesting higher diffusivities for these species. The top of the barriers can also be attributed to the closer approach of these species to anion-like regions in SiO_2 .

We estimate the thermal diffusion coefficient or diffusivity for the nitriding species using the Arrhenius law, given by

$$D(T) = D_0 \exp(-E_a/kT). \quad (1)$$

Here, the prefactor is defined by $D_0 = l^2 \nu / 6$ for a three-dimensional migration path, where l is the hopping distance between minima and ν is the attempt frequency, kT the Boltzmann constant times the temperature, and E_a is the highest energy barrier of the migration path. ν is calculated from the energy profile of each species at the interstitial site (approximately the zero distance in Fig. 4), using the harmonic ap-

TABLE I. Energy barriers (E_a), hopping distance between minima (l) and attempt frequencies (ν) as obtained from the migration energy profiles of Fig. 4. D_0 is the calculated prefactor coefficient of the diffusivities for each nitriding species.

Species	E_a (eV)	l (Å)	ν ($\times 10^{12} s^{-1}$)	D_0 ($\times 10^{-4} cm^2/s$)
NO	0.95	4.9	2.3	9.2
N_2	0.95	5.0	3.2	13.3
NH	0.48	2.8	3.7	4.8
N	0.60	3.9	3.4	8.6

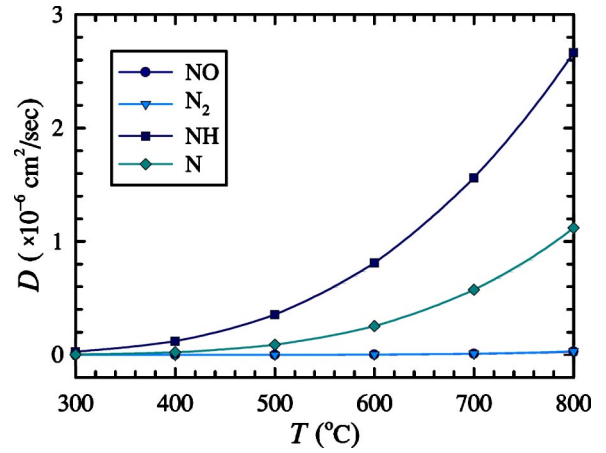


FIG. 5. Calculated diffusivities (D) of the nitriding species in α -quartz as a function of typical plasma assisted and thermal processing temperatures.

proximation, whereas E_a and l are obtained directly from the same figure. The values of these quantities as well as our results for the prefactor of each nitriding species are listed in Table I. It is worth pointing out that we have considered a very specific migration pathway through α -quartz. Other pathways may result in different migration barriers and diffusivities. In fact, recent calculations have shown major differences in the diffusivity of atomic hydrogen in different crystalline structures of SiO_2 .^{17,18} However, we find that our approach is valid to obtain informations on the relative diffusivities of the species under consideration.

Figure 5 shows the diffusivities of the nitriding species in α -quartz as calculated from Eq. (1), for a range of temperatures typically used in thermal and plasma assisted methods. Here we observe that NH and atomic N have the higher diffusivities in α -quartz with increasing temperatures as compared with NO and N_2 , which suggest that they would be the best thermally activated diffusing species in SiO_2 and the most efficient for Si- SiO_2 interface nitridation, as compared with NO and N_2 . According to our results, the ratio between NH and NO diffusivities at 800 °C is estimated to be $D_{NH}/D_{NO} \approx 90$. Assuming that NH and NO are the main diffusing species, our results agree well with the experimental finding of higher N concentrations at the interface obtained by thermal nitridation of SiO_2 in NH_3 as compared with thermal nitridation in N_2O .⁵

C. Spin-dependent diffusion reactions of NH and N in SiO_2

As mentioned above, NH in the triplet spin state does not react chemically with the SiO_2 network remaining inert at interstitial sites. However, singlet NH reacts easily with the oxide being incorporated into the network [see Fig. 3(a)]. Because of this spin-dependent reaction of NH with the SiO_2 network, we study the possibility that a diffusing NH may suffer a triplet-to-singlet spin conversion while approaching the oxide, resulting in its incorporation into the network. For this, we compute the PES along a pathway joining the equilibrium position of interstitial NH (the starting point) and a Si-O bond of the SiO_2 network, for both triplet and singlet

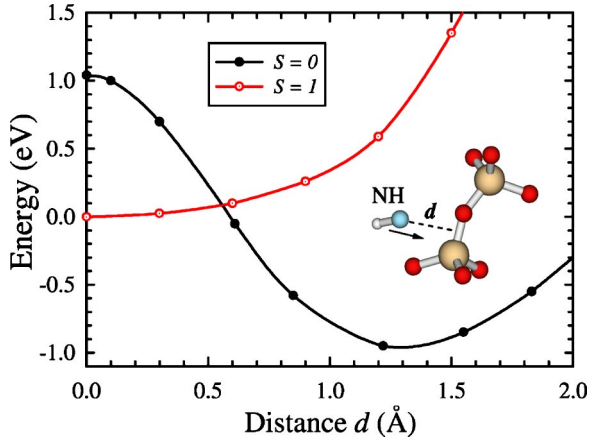


FIG. 6. Triplet ($S=1$) and singlet ($S=0$) total-energy curves along the reaction pathway (d in the inset figure) for the NH molecule approaching the SiO_2 network. The zero distance is the equilibrium position of NH in the largest interstitial site of α -quartz where its corresponding total energy is chosen as the zero energy of the system.

spin states, as shown in Fig. 6. The triplet PES in the figure is depicted along a direction perpendicular to the diffusion pathway shown in Fig. 4, however, both pathways intercept at the interstitial equilibrium configuration of NH (zero distance in Fig. 6). The probability that the system changes from the triplet to the singlet PES may be estimated by the Landau-Zener theory.¹⁹ This theory has been recently used to describe spin effects in the adsorption of O_2 in the $\text{Si}(001)$ surface²⁰ and the O_2 incorporation reaction in the Si-SiO_2 interface.¹⁵ Considering that the NH is initially in the triplet diffusion PES, and is evolving towards the crossing region with a velocity v , the probability for a conversion to the singlet PES (P_{ts}) may be approximated by

$$P_{ts} = 2[1 - \exp(-V^2/hv|F_1 - F_2|)], \quad (2)$$

where V is the triplet-to-singlet spin-orbit matrix element of NH ($X^3\Sigma^- \rightarrow b^1\Sigma^+$) of 65.1 cm^{-1} ,²¹ F_1 and F_2 are the slopes of the two PES at the crossing point and h is the Planck's constant. v is estimated from the NH center-of-mass thermal velocity at $800 \text{ }^\circ\text{C}$, a typical annealing temperature. F_1 and F_2 are obtained from the triplet and singlet curves at the crossing region (see Fig. 6). Thus, the probability for a triplet-to-singlet conversion is found to be $P_{ts} = 9.3 \times 10^{-4}$. This means that triplet NH in a single passage through the crossing point has a small probability to change to the singlet PES. However, as the system is thermally activated, many passages of NH through the crossing point will be performed. In order to quantify the spin-conversion events for NH molecules approaching the SiO_2 network at a given temperature, we estimate the ratio between the rate of NH following the triplet diffusion PES (Γ_t) and the rate of NH changing from triplet to singlet PES at the crossing point (Γ_{ts}). Assuming that the thermally-activated systems follow the Arrhenius law, the reaction rates can be written as

$$\Gamma_t = \Gamma_0^t \exp(-\Delta E_t/kT) \quad (3)$$

and

$$\Gamma_{ts} = \Gamma_0^{ts} [\exp(-\Delta E_p/kT)] \times P_{ts}. \quad (4)$$

Here, Γ_0^t is the attempt-frequency prefactor calculated from the diffusing energy profile of triplet NH (see Table I); Γ_0^{ts} is the prefactor calculated from the minimum of the triplet energy profile of Fig. 6, following the harmonic approximation ($\Gamma_0^{ts} = 3.2 \times 10^{12} \text{ s}^{-1}$); ΔE_t is the energy barrier for the triplet diffusion PES obtained from Fig. 4(b) ($\Delta E_t = 0.48 \text{ eV}$) and ΔE_p is the energy difference between the lowest-energy equilibrium configuration of the triplet NH and the crossing point, obtained from Fig. 6 ($\Delta E_p = 0.1 \text{ eV}$). For a temperature of $800 \text{ }^\circ\text{C}$, we obtain for our calculated P_{ts} that $\Gamma_t/\Gamma_{ts} \approx 16$, which indicates that NH will proceed preferentially along the triplet diffusion PES.

As the incorporation of NH into the oxide due to the spin exchange is very likely to occur (an average of one in 10^6 events), we estimate the reaction rates of three possible thermally activated diffusion mechanisms for an incorporated singlet-NH into the oxide at $800 \text{ }^\circ\text{C}$. These three rates must have similar prefactor since their respective PES evolve from the equilibrium geometry of an incorporated singlet-NH [see Fig. 3(a)]. We estimate the singlet prefactor (Γ_0^s) from the minimum of the singlet energy profile of Fig. 6, following the harmonic approximation ($\Gamma_0^s = 7.5 \times 10^{12} \text{ s}^{-1}$). Thus, the possible diffusion-reaction mechanisms of a singlet NH are: (i) *The incorporated NH diffuses along the SiO_2 network by a hopping mechanism.* The reaction rate can be estimated by Eq. (3), substituting ΔE_t by a calculated hopping energy barrier ($\Delta E_h = 2.2 \text{ eV}$). We find a hopping rate of $\Gamma_h = \Gamma_0^s (4.6 \times 10^{-11})$. (ii) *The incorporated NH is released from the network following the singlet PES.* The reaction rate can be estimated by

$$\Gamma_s = \Gamma_0^s [\exp(-\Delta E_s/kT)] \times (1 - P_{ts}), \quad (5)$$

where ΔE_s is the singlet PES energy barrier obtained from Fig. 6 ($\Delta E_s = 2.0 \text{ eV}$). We find that $\Gamma_s = \Gamma_0^s (4.0 \times 10^{-10})$. (iii) *The incorporated NH is released from the network changing from the singlet to the triplet PES at the crossing point.* The reaction rate can be estimated by Eq. (4), where ΔE_p is now the difference between the energies at the singlet-triplet crossing point and at the incorporated NH equilibrium configuration, obtained from Fig. 6 ($\Delta E_p = 1.05 \text{ eV}$). We find that $\Gamma_{st} = \Gamma_0^s (1.1 \times 10^{-8})$. According to these results, the most likely diffusion mechanism for an incorporated singlet NH in SiO_2 would be mediated by the reaction (iii), i.e., NH leaves the network changing from the singlet to the triplet PES at the crossing point and then diffuses through SiO_2 as a triplet NH. The two other mechanisms are less likely, as can be verified by the ratios $\Gamma_{st}/\Gamma_h \approx 240$ and $\Gamma_{st}/\Gamma_s \approx 28$.

Similarly to NH, we find a spin-dependent diffusion reaction for atomic N with the SiO_2 network. According to our results, the N atom in the ground quartet state does not react chemically with the network remaining at interstitial sites, whereas, in the doublet state, the N atom is incorporated between a Si-O bond, forming a strong bond with the O atom

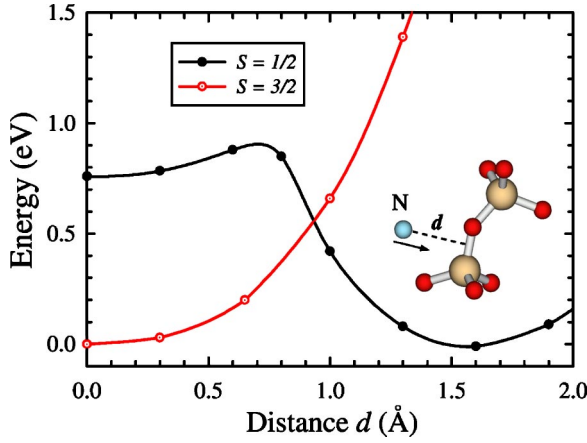


FIG. 7. Doublet ($S=1/2$) and quartet ($S=3/2$) total-energy curves along the reaction pathway (d in the inset figure) for the N atom approaching the SiO_2 network. The zero distance is the equilibrium position of the N atom in the largest interstitial site of α -quartz where its corresponding total energy is chosen as the zero energy of the system.

in a structure similar to the peroxy bridge of oxygens,²² as shown in Fig. 3(b). Therefore, we examine the possibility that the N atom, initially in the quartet state, changes the spin configuration to the doublet state, resulting in its incorporation into the oxide. Following the same procedure described above for NH, we compute the quartet and doublet PES for the N atom approaching the SiO_2 network. Our results are shown in Fig. 7. From Eq. (2) we obtain the probability for the spin conversion using for V the quartet-to-doublet spin-orbit matrix element of the N atom (${}^4P \rightarrow {}^2P$), obtained from spectroscopy data of 13.8 cm^{-1} . Thus, we find a quartet-to-doublet conversion probability $P_{qd}=1.6 \times 10^{-5}$. This probability corresponds to a single passage of the N atom through the crossing point. To estimate the number of spin-conversion events of thermally activated N atoms approaching the SiO_2 network, we calculate the ratio between the rate of N following the quartet diffusion PES (Γ_q) and the rate of N changing from quartet to doublet PES at the crossing point (Γ_{qd}). To calculate Γ_q we use Eq. (3) substituting ΔE_t by the energy barrier for the quartet diffusion PES obtained from Fig. 4(b) ($\Delta E_q=0.6 \text{ eV}$). The frequency prefactor (Γ_0^q) is obtained from the diffusing energy profile of quartet-N (see Table I). Γ_{qd} is estimated by Eq. (4) substituting P_{ts} by P_{qd} and using $\Delta E_p=0.6 \text{ eV}$, the difference between the energies at the interstitial site and at the quartet-doublet crossing point, obtained from Fig. 7. The quartet-to-doublet prefactor (Γ_0^{qd}) is calculated from the minimum of the quartet energy profile shows in Fig. 7, following the harmonic approximation ($\Gamma_0^{qd}=4.1 \times 10^{12} \text{ s}^{-1}$). This energy minimum corresponds to the equilibrium geometry of doublet N into the SiO_2 network, shown in Fig. 3(b). For a temperature of $800 \text{ }^\circ\text{C}$, we find that $\Gamma_q/\Gamma_{qd} \approx 5 \times 10^4$. This result indicates that the N atom will most likely proceed along the quartet PES, i.e., it diffuses through the SiO_2 essentially without reacting with the network.

Although very unlikely, the reaction of a doublet N with the oxide due to the spin exchange may also occur. There-

fore, we estimate the rates of three possible thermally activated diffusion mechanisms for a doublet N, once it is incorporated into the oxide at $800 \text{ }^\circ\text{C}$. These three rates must have similar prefactor since their respective PES evolve from the equilibrium geometry of an incorporated doublet-N [see Fig. 3(b)]. We estimate the doublet prefactor (Γ_0^d) from the minimum of the doublet energy profile of Fig. 7, following the harmonic approximation ($\Gamma_0^d=6.9 \times 10^{12} \text{ s}^{-1}$). Thus, the possible diffusion-reaction mechanisms of a doublet-N are: (i) *The incorporated N diffuses through the SiO_2 network by a hopping mechanism.* From Eq. (3), substituting ΔE_t by the calculated hopping energy barrier ($\Delta E_h=1.8 \text{ eV}$), we find $\Gamma_h=\Gamma_0^d(3.5 \times 10^{-9})$. (ii) *The incorporated N is released from the network following the doublet PES.* From Eq. (5), substituting ΔE_s by the doublet PES energy barrier, obtained from Fig. 7 ($\Delta E_d=0.9 \text{ eV}$), and P_{ts} by P_{qd} , we find $\Gamma_d=\Gamma_0^d(5.9 \times 10^{-5})$. (iii) *The incorporated N is released from the network, changing from the doublet to the quartet PES at the crossing point.* From Eq. (4), substituting P_{ts} by P_{qd} and using $\Delta E_p=0.6 \text{ eV}$, the difference between the energy of quartet N at the interstitial site and at the quartet-to-doublet crossing point, obtained from Fig. 7, we find $\Gamma_{dq}=\Gamma_0^d(2.4 \times 10^{-8})$. Therefore, if a N atom is incorporated into the oxide by a quartet-to-doublet spin exchange, a rare event, it will be released from the network following the doublet PES, according to the reaction (ii). However, as the incorporation reaction of the doublet N is exothermic, it will be reincorporated in the network if the timescale for relaxation back to the quartet ground state is long enough. Finally, we find that the other two possible reactions are very unlikely as can be verified by the ratios $\Gamma_d/\Gamma_h \approx 1.7 \times 10^4$ and $\Gamma_d/\Gamma_{dq} \approx 2.5 \times 10^3$.

IV. CONCLUSIONS

We conclude that because of the ionic character of SiO_2 , charged species are bound to the network by chemical and electrostatical interactions, where positive (negative) species tend to attach to oxygen (silicon) atoms, forming strong bonds with binding energies as high as 3 eV . This suggests a mechanism for the N incorporation in bulk SiO_2 observed in plasma assisted method, which would be associated to charged species surviving the first stages of the incorporation reactions occurring at the surface. Of course, these charged species may also transfer the charge to the network becoming neutral. According to our results, neutral species do not react chemically with the network remaining at interstitial sites, therefore, they would be diffusing species in SiO_2 able to reach the Si-SiO₂ interface.

We estimate the diffusivities of neutral species through α -quartz. Our results show that NH and atomic N have increasing diffusivities with temperature, and the highest one among the nitriding species, suggesting that they would be efficient for near interface nitridation. This result is in good agreement with the finding of high N concentration at the Si-SiO₂ interface obtained by thermal processing in NH_3 . On the other hand, NO and N_2 show relatively constant diffusivities in α -quartz for the same range of temperatures. This result is also in good agreement with the finding of relatively

low N concentration at the Si-SiO₂ interface obtained by thermal processing in N₂O, which is the main source of NO and N₂ species.

We also study the incorporation reaction of NH and atomic N with the SiO₂ network driven by a spin exchange mechanism. We find that, for a typical annealing temperature ($T=800$ °C), a NH molecule diffusing through the triplet PES will have, on average, one in sixteen possibilities to be incorporated into the network by a triplet-to-singlet conversion. The incorporated singlet NH will most likely return to the triplet PES after an inverse spin conversion. We also find that atomic N may be incorporated into the network by a quartet-to-doublet conversion while diffusing through the

quartet PES, however, only an average of one in 5×10^4 events will be successful. If this rare event occurs, the incorporated N will be released from the network following the doublet PES and, subsequently, reincorporated into the network due to the doublet exothermic process. However, this mechanism will be valid if the timescale for the relaxation to the quartet ground state is long enough.

ACKNOWLEDGMENTS

This work was supported by FAPESP and CNPq. We also would like to thank CENAPAD-SP for computer time.

*Electronic address: wmomunoz@if.usp.br

¹M. L. Green, E. P. Gusev, R. Degraeve, and E. L. Garfunkel, *J. Appl. Phys.* **90**, 2057 (2001).

²E. Cartier, D. A. Buchanan, and G. J. Dunn, *Appl. Phys. Lett.* **64**, 901 (1994).

³D. Wristers, L. K. Han, T. Chen, H. H. Wang, and D. L. Kwong, *Appl. Phys. Lett.* **68**, 2094 (1996).

⁴K. A. Ellis and R. A. Buhrman, *IBM J. Res. Dev.* **43**, 287 (1999).

⁵I. J. R. Baumvol, *Surf. Sci. Rep.* **49**, 5 (1999).

⁶H. C. Lu, E. P. Gusev, E. Garfunkel, B. W. Busch, T. Gustafsson, T. W. Sorsch, and M. L. Green, *J. Appl. Phys.* **87**, 1550 (2000).

⁷K. Watanabe and T. Tatsumi, *Appl. Phys. Lett.* **76**, 2940 (2000).

⁸E. P. Gusev, D. A. Buchanan, P. Jamison, T. H. Zabel, and M. Copel, *Microelectron. Eng.* **48**, 67 (1999).

⁹W. Orellana, *Appl. Phys. Lett.* **84**, 933 (2004).

¹⁰S. Jeong and A. Oshiyama, *Phys. Rev. Lett.* **86**, 3574 (2001).

¹¹P. Hohenberg and W. Kohn, *Phys. Rev.* **136**, B864 (1964); W. Kohn and L. J. Sham *ibid.* **140**, A1133 (1965).

¹²P. Ordejón, E. Artacho, and J. M. Soler, *Phys. Rev. B* **53**,

R10 441 (1996); J. M. Soler, E. Artacho, J. D. Gale, A. Garcia, J. Junquera, P. Ordejón, and D. Sánchez-Portal, *J. Phys.: Condens. Matter* **14**, 2745 (2002).

¹³N. Troullier and J. L. Martins, *Phys. Rev. B* **43**, 1993 (1991).

¹⁴J. P. Perdew, K. Burke, and M. Ernzerhof, *Phys. Rev. Lett.* **77**, 3865 (1996).

¹⁵W. Orellana, A. J. R. da Silva, and A. Fazzio, *Phys. Rev. Lett.* **90**, 016103 (2003).

¹⁶W. Orellana, A. J. R. da Silva, and A. Fazzio, *Phys. Rev. Lett.* **87**, 155901 (2001).

¹⁷A. Bongiorno, L. Colombo, and M. I. Trioni, *J. Non-Cryst. Solids* **216**, 30 (1997).

¹⁸B. Tuttle, *Phys. Rev. B* **61**, 4417 (2000).

¹⁹C. Zener, *Proc. R. Soc. London, Ser. A* **137**, 696 (1932).

²⁰K. Kato, T. Uda, and K. Terakura, *Phys. Rev. Lett.* **80**, 2000 (1996).

²¹D. R. Yarkony, *J. Chem. Phys.* **92**, 320 (1990).

²²D. R. Hamann, *Phys. Rev. Lett.* **81**, 3447 (1998).